Available online at www.sciencedirect.com
SCIENCE DIRECT®
International Journal of Mass Spectrometry 233 (2004) 343–354
International Journal of Mass Spectrometry
www.elsevier.com/locate/ijms

Elementary processes at the origin of the generation and dynamics of multiple double layers in DP machine plasma

Codrina Ioniţă*, Dan-Gheorghe Dimitriu[1], Roman W. Schrittwieser

Department of Ion Physics, University of Innsbruck, A-6020 Innsbruck, Austria

Received 24 September 2003; accepted 13 January 2004

To Tilmann Märk on the occasion of his 60th birthday, a true colleague and friend, supportive, full of inspiration, encouragement and energy.

Abstract

We report new results on the generation and dynamics of multiple double layers (MDLs) in front of a positively biased electrode immersed in plasma. The phenomenon appears as a set of concentric luminous shells with different intensities, attached to the electrode. The static current–voltage characteristic of the electrode shows a number of jumps of the current, each of them associated with hysteresis, which proves the role of excitation and ionization processes in the appearance and dynamics of such a strongly non-linear potential structure. The recorded time series of the current oscillations and the associated FFTs elucidate that initially each of the double layer structures performs a proper non-linear dynamical process, with the corresponding current oscillations being uncorrelated. This uncorrelation leads to the creation of flicker noise, identified in the power spectrum of the current oscillations. At high voltages on the electrode the dynamics of the double layers become correlated and the flicker noise disappears. The non-linear dynamical analysis of the signals yields information about the state space dynamics of our plasma system.
© 2004 Elsevier B.V. All rights reserved.

Keywords: Multiple double layers; Non-linear oscillations; Excitation; Ionization; Flicker noise

1. Introduction

Double layers (DLs) [1] in plasma were intensively investigated during the last decades because of their frequent occurrence in almost all possible plasma devices: tokamaks [2,3] or spheromaks [4], thermionic converters [5], Q-machines [6–8], double plasma (DP) and triple plasma (TP) machines [9,10]. Also in natural plasmas DLs have been observed or postulated: auroras [11,12], solar flares [13], ball lightnings [14,15]). In many applications their bistable behaviour is suitable: e.g., for fast switches, quantum photodetectors or high-frequency generators. DLs are non-linear potential structures, consisting of two adjacent layers of positive and negative space charges, in which the potential jumps, thereby creating an electric field. A usual DL needs at least four populations of charge carriers: (i) on the low potential side free electrons, which can be accelerated through the DL towards the high potential side, (ii) on the low potential side trapped ions, which are reflected back by the DL, (iii) on the high potential side trapped electrons, which are reflected back by the DL, (iv) on the high potential side free ions, which are accelerated through the DL towards the low potential side.

One common way to obtain a DL structure is to positively bias an electrode immersed in a plasma being in thermodynamic equilibrium. In this case, a complex space charge configuration (CSCC) in form of a quasi-spherical luminous plasma body attached to the electrode is obtained. This type of CSCC was named anode glow [16] and more recently fireball [17]. Experimental investigations revealed that such a CSCC consists of a positive “nucleus” (an ion-rich plasma) surrounded by a nearly spherical DL [17–20]. The potential drop across the DL is almost equal to the ionization potential of the background gas atoms.

Under certain experimental conditions (plasma density, gas nature and pressure, electron temperature) a more complex structure in form of two or more subsequent DLs was

* Corresponding author.
E-mail addresses: codrina.ionita@uibk.ac.at (C. Ioniţă), dimitriu@uaic.ro (D.-G. Dimitriu), roman.schrittwieser@uibk.ac.at (R.W. Schrittwieser).
[1] Present address: Faculty of Physics, University “Al. I. Cuza”, RO-6600 Iasi, Romania.

1387-3806/$ – see front matter © 2004 Elsevier B.V. All rights reserved.
doi:10.1016/j.ijms.2004.01.009

observed [21–28]. It appears as several (more than five [26]) bright and concentric plasma shells attached to the anode of a glow discharge. The successive DLs are precisely located at the abrupt changes of luminosity between two adjacent plasma shells. Langmuir probes measurements emphasized that the axial profile of the plasma potential has a stair steps shape, with potential jumps close to the ionization potential of the used gas [26].

In this paper we report on experimental results concerning the generation and dynamics of multiple double layers (MDLs) in a different experimental geometry. Usually such a structure was obtained at the anode of a glow discharge. We generate MDLs at a positively biased electrode immersed in a DP-machine plasma. This experimental arrangement presents many advantages, the most important of them is that we can analyse the elementary processes, which occur during the appearance and the onset of MDLs without any change in the discharge plasma parameters.

The analysis of the experimental results proves the important role of elementary processes for the formation of a MDL. These are mainly electron impact excitation and ionization processes, which determine the appearance of negative and positive space charges, respectively, spatially well separated because of the dependence of the respective cross-sections on the kinetic electron energy, which varies along the MDL according to the potential profile. When the potential drop between the opposite space charges attains the ionization potential of the gas, a DL structure is formed. The DL can accelerate thermal electrons from the surrounding plasma to energies large enough to produce further excitation and ionization processes. A further increase of the voltage on the electrode causes an increase of the potential drop across the DL and, consequently, an increase of the space charges. In this way the DL is driven away from the electrode and, at a certain distance, it disrupts, and consequently the trapped electrons and ions are freed. The disruption of one DL triggers the appearance of a new DL in front of the electrode, which starts its own dynamics, the process becoming a periodical one [29].

In this way, on the time average, always a DL exists in front of the electrode, but in a dynamic equilibrium. If the plasma density and the gas pressure are large enough, a second quasistable DL structure can appear. When the two DL structures start their proper dynamics at different frequencies, uncorrelated phenomena will appear in the plasma system, which lead to the creation of flicker noise in the current oscillations power spectrum. This phenomenon was already associated with the uncorrelated dynamics of DL structures [30,31]. At large values of the voltage on the electrode the two DL dynamics become correlated, wherefore only one peak remains in the power spectrum and the flicker noise disappears.

All these phenomena can be observed experimentally in the static current–voltage characteristic of the electrode and in the time series of the current oscillations with the associated power spectra. A comprehensive non-linear dynamical analysis of the recorded signals, including the reconstruction of the state space and the wavelet decomposition [32], gives us a broad picture of the state space dynamics of the plasma system and offers an excellent insight into the mechanism of the investigated phenomena.

2. Brief theory of spherical double layers

The DL structure is maintained by the equilibrium between the ions produced inside the structure and the ion loss from the structure. If we assume a nearly spherical structure (excepting a small region where the DL is attached to the electrode), the rate of ion production within the structure is [17]:

$$\frac{\mathrm{d}N_\mathrm{i}}{\mathrm{d}t} = 4\pi\left(\frac{D}{2}\right)\Gamma_\mathrm{e}\sigma_\mathrm{i}DN \tag{1}$$

where D is the diameter of the structure, Γ_e is the electron flux into the structure, σ_i is the ionization cross-section of the neutral gas, corresponding to an energy slightly above the ionization energy and N is the neutral gas density. The rate of ion loss from the DL is:

$$\frac{\mathrm{d}N_\mathrm{i}}{\mathrm{d}t} = 4\pi\left(\frac{D}{2}\right)\Gamma_\mathrm{i} \tag{2}$$

where Γ_i is the ion flux from the structure. For a stable structure, the two rates defined above must be equal. This means:

$$\Gamma_\mathrm{i} = \Gamma_\mathrm{e}\sigma_\mathrm{i}DN \tag{3}$$

The electron and ion fluxes, respectively, are related by the Langmuir condition [33]:

$$\Gamma_\mathrm{e} = \left(\frac{m_\mathrm{i}}{m_\mathrm{e}}\right)^{12}\Gamma_\mathrm{i} \tag{4}$$

where m_i and m_e are the ion and the electron masses, respectively. By inserting Eq. (4) into Eq. (3) we can estimate the diameter of the structure:

$$D = \frac{1}{\sigma_\mathrm{i}N}\left(\frac{m_\mathrm{e}}{m_\mathrm{i}}\right)^{12} \tag{5}$$

For our experimental conditions, using Eq. (5), we obtain $D \cong 7.65\,\mathrm{cm}$, which is a very good estimate of the experimentally observed values for the diameter of the DL structure, which in our case lies between 3.5 and 12 cm.

The period of the current oscillations is proportional to the ionization time, given by [17]:

$$t_\mathrm{ioniz} = \frac{1}{N\sigma_\mathrm{i}v_\mathrm{e}} \tag{6}$$

where v_e is the electron velocity:

$$v_\mathrm{e} = \sqrt{\frac{2\mathrm{e}V_\mathrm{DL}}{m_\mathrm{e}}} \tag{7}$$

with V_{DL} being the voltage across the double layer. This delivers a frequency of:

$$f \cong N\sigma_i\sqrt{\frac{2eV_{DL}}{m_e}} \quad (8)$$

For $V_{DL} = 20\,V$, $\sigma_i = 6 \times 10^{-17}\,cm^2$ [34] and, using Eq. (8), we obtain $f = 19.2\,kHz$, which is a good estimate of our experimental values, which lie between 2 and 45 kHz, approximately.

3. Experimental set-up

The experiments were performed in the DP-machine of the University of Innsbruck, Austria, schematically presented in Fig. 1. The DP-machine consists of a cylindrical vacuum vessel of 45 cm diameter and a length of 90 cm. The vacuum vessel is divided into two parts by a fine mesh grid that extends over the entire cross-section of the inner cylinder. The grid is electrically isolated from the wall and can be biased arbitrarily with respect to ground. The two parts of the machine are named source chamber (left-hand side in the Fig. 1) and target chamber (right-hand side in the Fig. 1), respectively. The source chamber has an additional inner wall, which is isolated from the vessel wall and can thus also be biased arbitrarily with respect to ground. In both chambers there are filaments that act as hot cathodes for glow discharges, which are produced independently in argon at a pressure of about 10^{-4} mbar. The walls of the two chambers act as the anodes of the discharges. On the inner walls of the vacuum vessels small permanent magnets with alternate polarity are fixed, forming a picket-fence magnetic field, which supports the plasma confinement. Because of the small dimensions, the filament collects only a negligible part of the ions, most of them diffusing to the centre of the vacuum cylinder. The positive space charge will attract many electrons to this region. In this way, a plasma with a high degree of ionization is created.

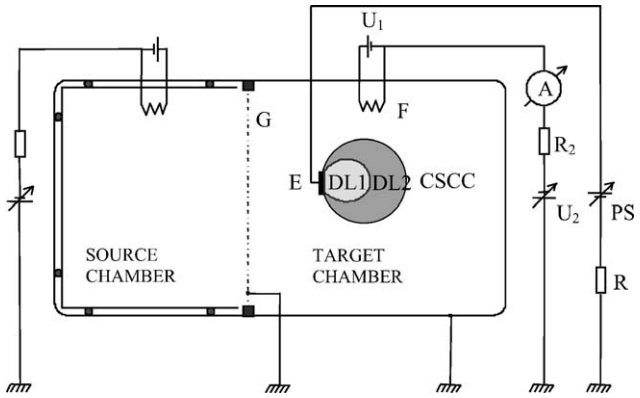

Fig. 1. Schematic of the Innsbruck DP-machine. G: grid, F: filaments, E: electrode, PS: power supply, R: load resistor.

In our experiments we used only the target chamber of the DP-machine. The plasma was pulled away from its steady state by gradually increasing the voltage to a circular tantalum disk electrode (E in Fig. 1) with 2 cm diameter. The voltage is delivered by a power supply (PS in Fig. 1) through a load resistor $R = 500\,\Omega$. The background argon pressure was $p \cong 5 \times 10^{-3}$ mbar and the plasma density $n \cong 10^{10}$–$10^{11}\,cm^{-3}$. An *XY* recorder was used to register the static current–voltage characteristic of E. The ac component of the electrode current was recorded with by a digital computer-controlled oscilloscope. The plasma potential was measured by an emissive probe in the dynamic regime, using a box-car averaging technique.

4. Experimental results

Fig. 2 shows the static current–voltage ($I_E - V_E$) characteristic of the electrode E obtained by gradually increasing and decreasing the voltage from the PS (V_{PS}), for the case where in front of E two luminous plasma shells were obtained. The small letters indicate the positions on the $I_E - V_E$ characteristic, where sudden changes of the current occur. Between these current jumps, the AC components of I_E and the FFTs of them have been recorded, either during the increase or during the subsequent decrease of V_E (Figs. 3 and 4, respectively).

By gradually increasing V_{PS}, the $I_E - V_E$ characteristic follows the branch a → b, in which I_E increases proportionally to V_E (the ohmic branch of the characteristic). A luminous sheet appears in front of E when V_E approaches the value marked by b. Its luminosity and extension increase simultaneously with V_E. On this branch of the $I_E - V_E$ characteristic the collected current is stable, with no oscillations (see Figs. 3(i) and 4(i), respectively). When V_E reaches the value corresponding to b, the luminous sheet suddenly expands into a spherical plasma configuration (a CSCC) attached to E. Simultaneously, the current I_E abruptly increases (jump b → c), and

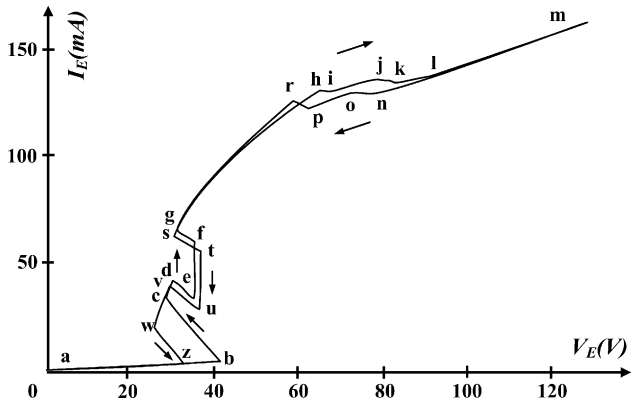

Fig. 2. Static upward and downward current–voltage characteristic of the electrode E, for argon pressure $p = 5 \times 10^{-3}$ mbar, plasma density $n = 10^{10}$–$10^{11}\,cm^{-3}$ and a load resistor $R = 500\Omega$.

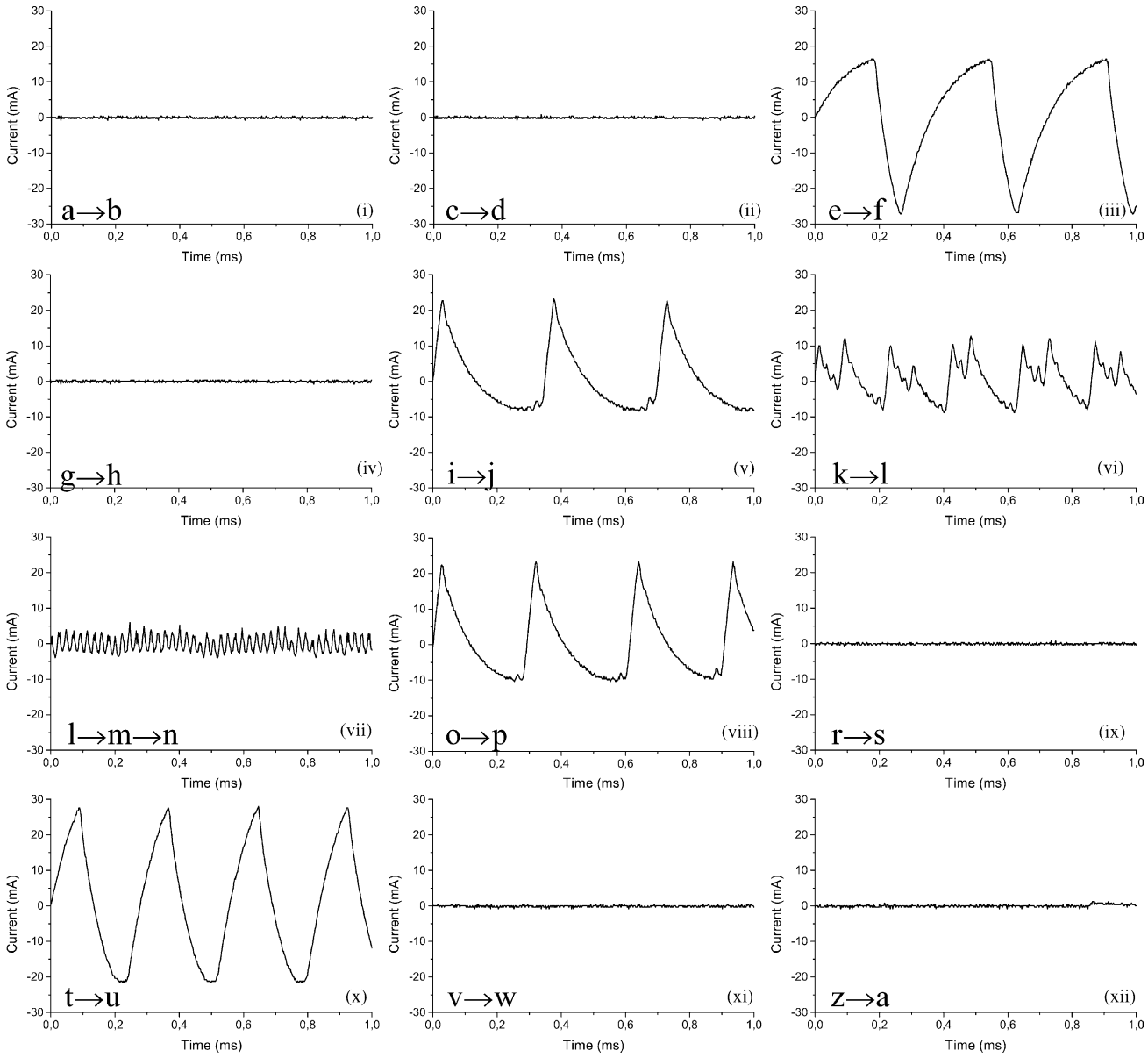

Fig. 3. Time series of the AC components of the electrode current, taken on the static characteristic branches between current jumps.

then remains stable (see Figs. 3(ii) and 4(ii), respectively). When V_{PS} is further increased (branch c → d) the current I_E gradually increases simultaneously with the extension of a stable CSCC. When V_E reaches the value corresponding to d, the current I_E quickly decreases and simultaneously becomes time dependent (see Figs. 3(iii) and 4(iii), respectively). On the branch e → f the frequency of the I_E oscillations depends almost proportionally on the mean value of I_E (the value from the static $I_E - V_E$ characteristic) (see Fig. 5). The oscillations are strongly non-linear, with more than 25 harmonics appearing in the power spectrum. When V_E reaches the value corresponding to point f, the current I_E quickly increases (jump f → g) and becomes stable (see Figs. 3(iv) and 4(iv), respectively). Simultaneously, a second luminous spherical sheet appears, surrounding the first one. Note that in this moment the diameter of the first luminous body decreases from about 5 cm to about 3.5 cm.

A further increase of V_E (branch g → h) leads to an increase of the MDLs luminosity and of its diameter. When V_E reaches the value corresponding to point h, the MDL starts a complex dynamic behaviour. First, simultaneously with the downward jump h → i, the current again becomes time dependent (see Figs. 3(v) and 4(v), respectively). In the power spectrum two fundamental frequencies appear, one of about 2.75 kHz corresponding to the dynamics of the inner sheet, and one of about 40 kHz corresponding to the dynamics of the outer sheet. The two dynamics are uncorrelated, giving rise to flicker noise (see the power spectrum in logarithmic co-ordinates from Fig. 6(i)) [35–37]. The shape of the current oscillations (Fig. 3(v)) shows that the dynamics

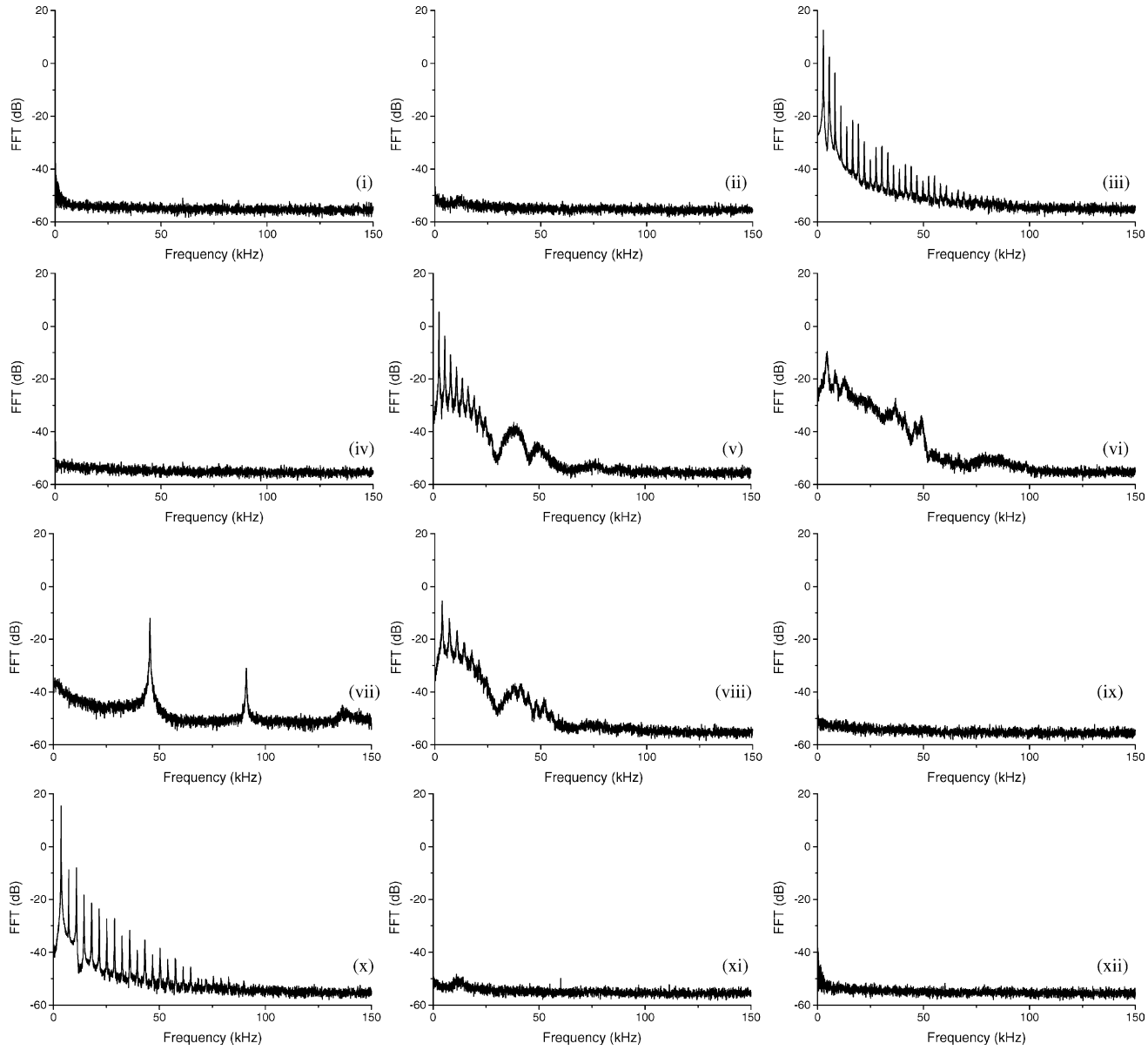

Fig. 4. FFTs of the AC components of the current from Fig. 3.

of the inner sheet is dominant. After the I_E jump j → k, the shape of the current oscillations changes (see Figs. 3(vi) and 4(vi), respectively). The dynamics of the outer sheet tends to become dominant but the dynamics of the two sheets remain uncorrelated and the flicker noise is still present (see Fig. 6(ii)). When V_E reaches the value corresponding to point l, the dynamics of the two sheets become correlated, and the flicker noise disappears. In the power spectrum only one fundamental frequency remains and the amplitude of the oscillations decreases (see Figs. 3(vii) and 4(vii), respectively). In this region of the $I_E - V_E$ characteristic the axial profile of the plasma potential was recorded with the help of an emissive probe and a box-car averaging technique, using I_E as reference signal. The results are shown in the Fig. 7, were V_E was about 80 V. We can observe two potential jumps, one at about 4.5 cm from E and the second at about 9.5 cm from E. The amplitudes of these jumps are about 15 and 19 V, respectively, close to the ionization potential of argon. We notice that the plasma potential outside the MDL is about 40 V, which for these conditions is in keeping with recent findings [20]. When V_E is gradually decreasing we observe that all current jumps are subject to hysteresis effects. In Figs. 3(viii–xii) and 4(viii–xii), respectively, the ac components of I_E and their FFTs are shown, recorded during the decrease of V_E on the all branches located between current jumps.

5. Non-linear dynamical analysis

The non-linear dynamical analysis provides us with powerful tools for analysing the evolution of a non-linear

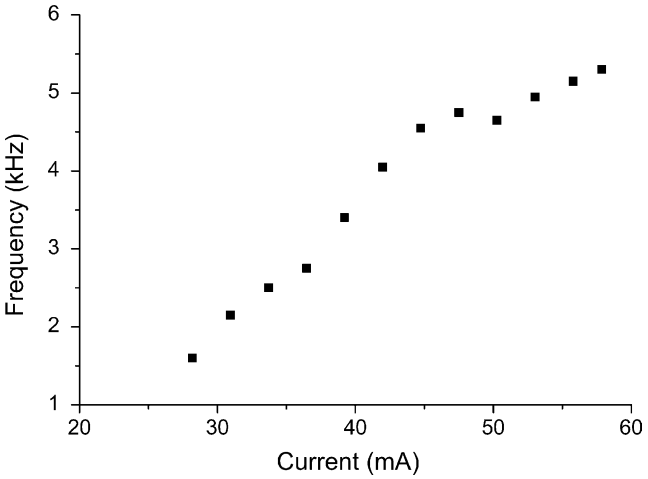

Fig. 5. Frequency of the current oscillations vs. the DC component of the electrode current, on the branch e → f of the static current–voltage characteristic (Fig. 2).

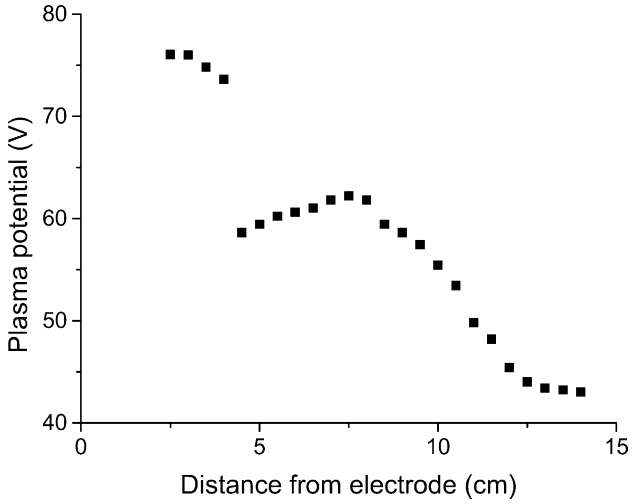

Fig. 7. Axial profile of the plasma potential in front of the electrode E.

system such as histograms, Fourier spectra, state space plots, Poincaré maps, Lyapunov exponents, attractor reconstruction, wavelet decomposition, and so forth. To apply some of these methods to our plasma system, we have recorded the AC components of the I_E with a sampling rate of 500 kHz, delivering 15,000 points in 0.03 s.

To reconstruct the attractors of the system dynamics in the state space, we have used the method proposed by Packard et al. [38], Ruelle [39] and Takens [40], extensively described in ref. [41]. The results are shown in the Fig. 8. We remark the limit cycle shapes of the attractors in Fig. 8(iii), (v), (vii), (viii) and (x), respectively. These are characteristic for periodical signals [42]. As a matter of course, the cycles are very deformed because of the strongly non-linear character of the oscillations. The point-attractors in Fig. 8(i), (ii), (iv), (ix), (xi) and (xii), respectively, are stable nodes of the well type. This explains why the non-oscillatory state of the double layer structure is extremely stable to any external fluctuations (potential of the electrode, electron or ion temperatures, electrical resistance, plasma density, gas pressure, etc.). The attractor of Fig. 8(vi) is strange, with a very complicated geometrical shape and a fractal dimension.

Fig. 9.1 and 9.2 show the wavelet decomposition of the AC component of I_E, obtained by a method extensively described in ref. [32]. The decomposition was made on 12 octaves and the used wavelet functions were of Daubechies type.

The wavelet analysis is an important refinement and expansion of the Fourier analysis. Whereas the latter investigates a signal globally, the wavelet analysis looks into the signal locally. It not only gives the main frequencies, but also indicates when they occur and what their duration is. The wavelet transform is sometimes called mathematical microscope [43] because it allows to “zoom” in and out at any desired magnification and at any point of time in the signal. Using the wavelet analysis we can investigate complex

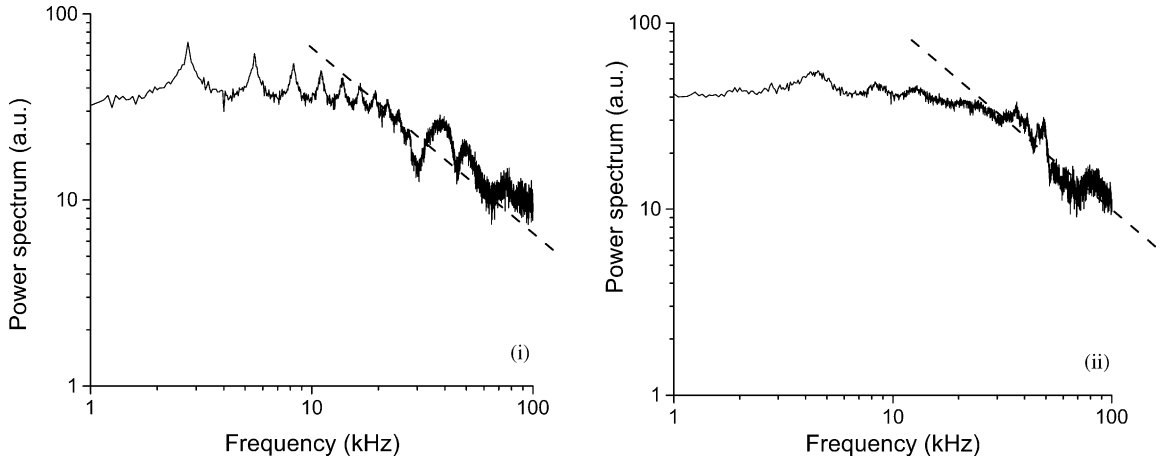

Fig. 6. Power spectrum of the AC components of the electrode current from Fig. 3 (vi) and (vii), respectively, where the dynamics of the two DLs are uncorrelated.

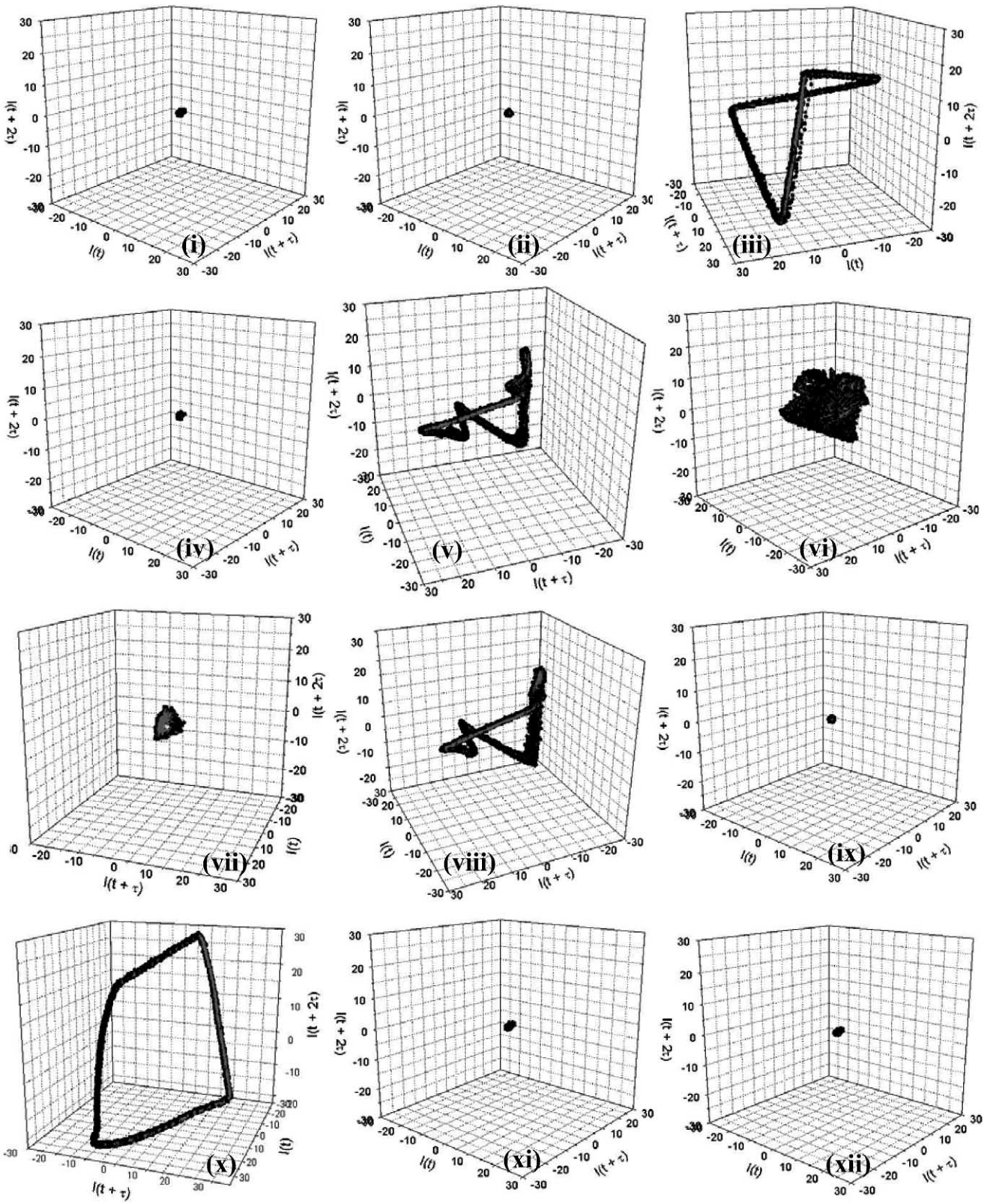

Fig. 8. Attractors of the plasma system dynamics, reconstructed from the AC components of the electrode current from Fig. 3.

signals like those of Fig. 3(vi). Thus, the wavelet decomposition of Fig. 9.1(vi) reveals the existence of periodic signal "islands", with different frequencies and amplitudes, interrupted by noisy regions.

6. Discussion

The appearance of a CSCC in form of a spherical DL in front of a positive biased electrode immersed in plasma

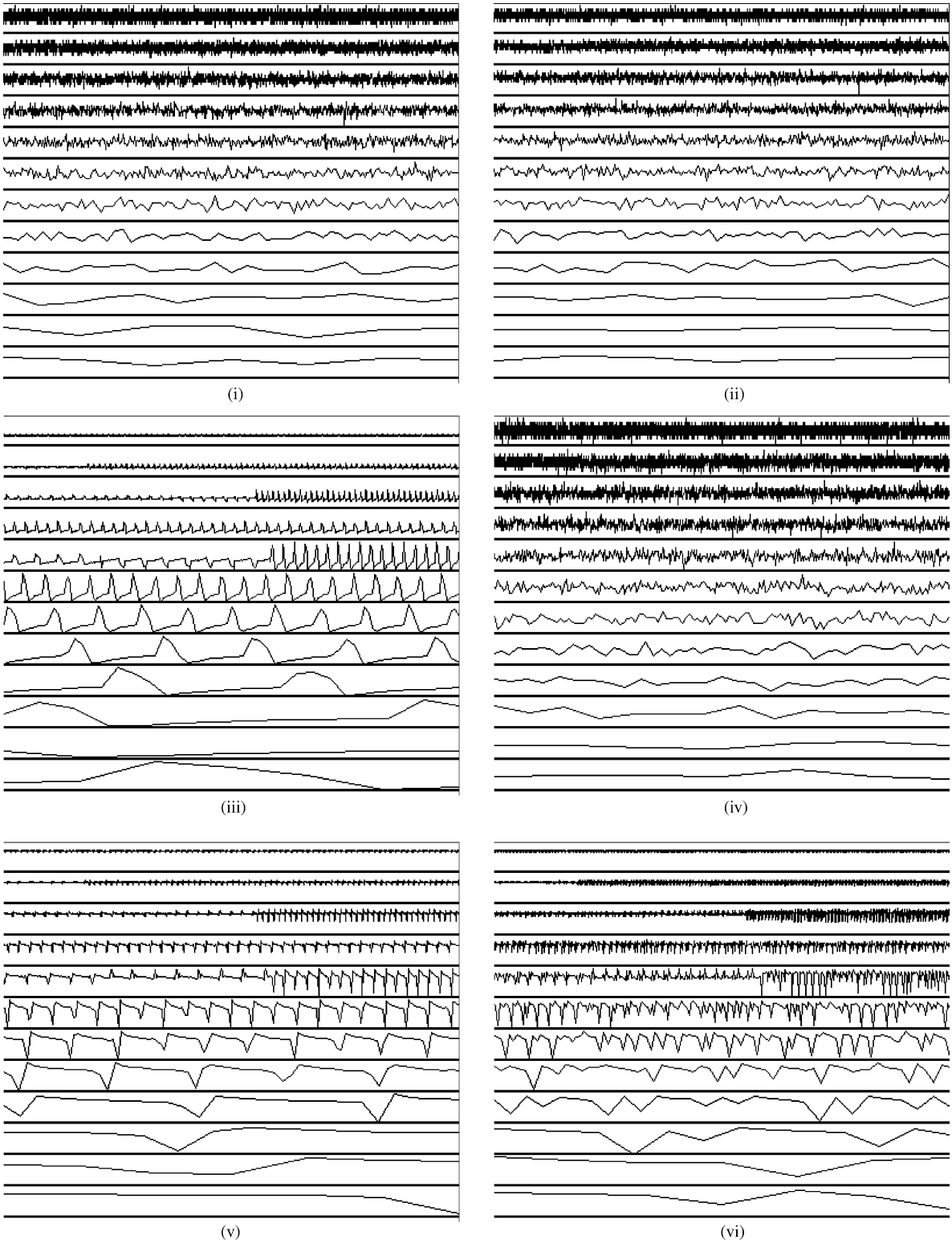

Fig. 9. Wavelet decomposition on 12 octaves of the AC component of the electrode current from Fig. 3.

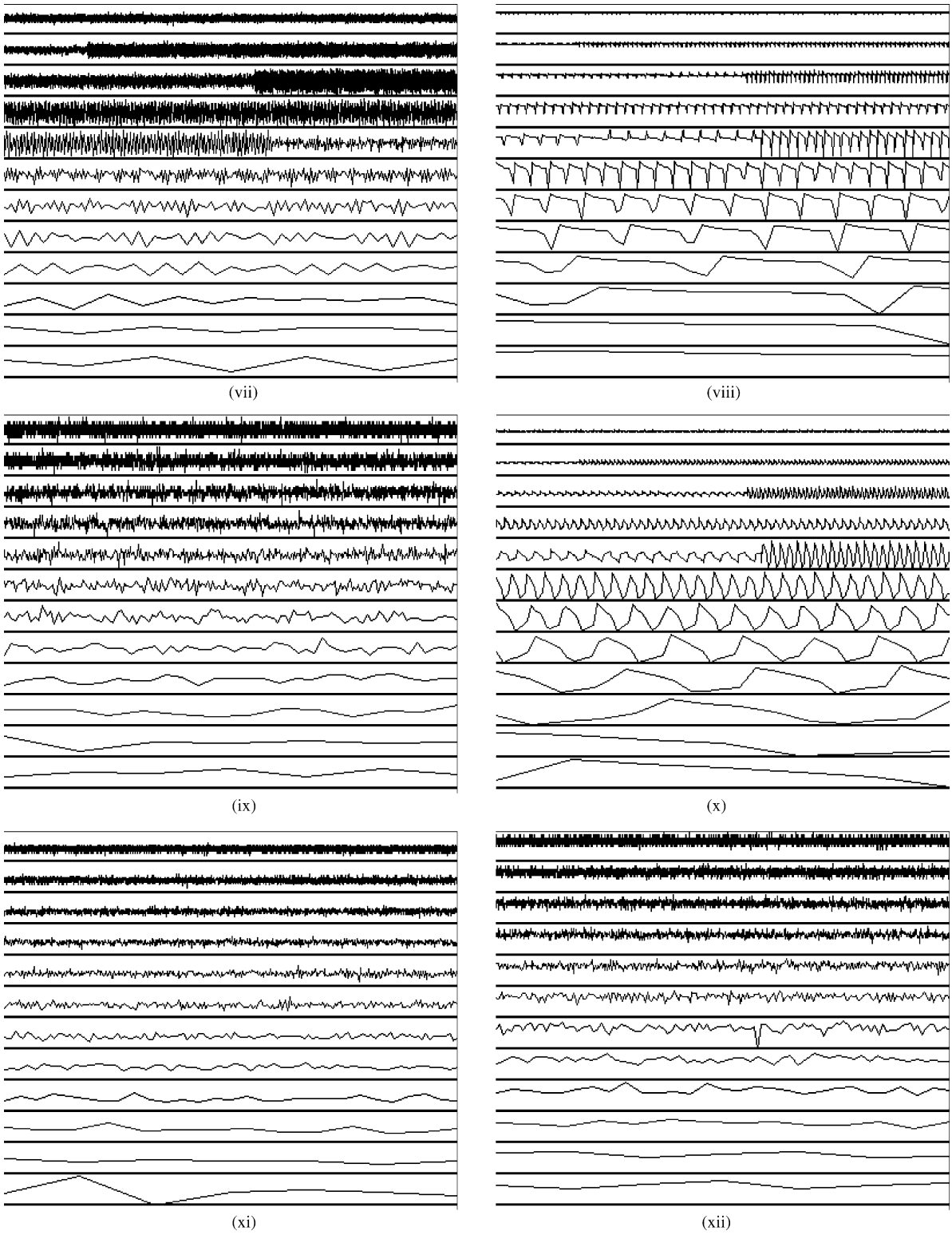

Fig. 9. (*Continued*).

is a well-known phenomenon [9,16,17]. So, here we will concentrate on the explanation of the elementary processes, which occur at the beginning of the generation and dynamic of the second DL of the MDL. When a positive bias is applied on the electrode immersed in plasma, the electrons from the neighbouring region are accelerated towards it. This region is extended with the increase of the voltage on E. The appearance of the luminous sheet near E on the a → b branch of the $I_E - V_E$ characteristic, proves the occurrence of excitations processes of gas atoms there.

Probe measurements complemented by spectral investigations show that a net negative space charge is formed in the region where light is emitted [15,44]. This space charge is formed by accumulation of those electrons that have lost their momentum after neutral impact excitations. The position of the net negative space charge is in front of E, in the region where the excitation cross-section of the gas atoms suddenly increases. The electrons that have not undergone excitation reactions obtain more kinetic energy eventually sufficient to perform impact ionization reactions of the gas atoms. The electrode E quickly collects the electrons that have performed excitation reactions and those resulting after impact ionizations, so that a plasma enriched in positive ions (a net positive space charge) appears in front of E. Simultaneously with its development, electrostatic forces begin to act as long-range correlations between the two adjacent opposite net space charges. Consequently, the opposite net space charges transforms into a double space charge configuration. This double space charge configuration supports a local potential drop, the value of which depends on the amount of electrons and positive ions located at its two sides and, implicitly, on the excitation and ionization rates.

When the potential drop over the DL reaches the ionization potential of the gas atoms, an amplification of the charge production takes place, which determines the current jump b → c on the $I_E - V_E$ characteristic (Fig. 2). Simultaneously, the electrostatic forces between the two opposite space charges suddenly increase and become dominant with respect to the external forces. Consequently, the space charge configuration performs a fast transition into a state characterized by a local minimum of the potential energy, i.e., a state, in which its shape becomes spherical. In the voltage range c → d, the stability of the DL is ensured by a balance between the charge losses by recombination and diffusion, and the charges accumulated and created in adjacent regions. The further increase of the voltage on E produces a shift of the DL away from E. In this way, the electrons can be accelerated between the DL and E to energies large enough to produce excitations of the neutrals, and a negative space charge is developed. This negative space charge acts as a barrier for the current, reducing the flux of electrons through the DL (jump d → e in Fig. 2). Thus, the balance needed for the DL existence is perturbed and the DL disrupts. The electrons trapped in the DL become free and move as a bunch toward E, arriving in the region where a new DL is the growing phase. In this way, the excitation and ionization rates suddenly increase at the value, for which the new DL at the CSCC edge starts the detachment process. The phenomenon becomes a periodical one, which is shown by the presence of oscillations in the current collected by E (Fig. 3(iii)).

The presence of such spatiotemporal phenomena was experimentally verified by plotting space–time diagrams [45]. The increase of I_E on the branch e → f of the static characteristic (Fig. 2) leads to an increase of the electron flux through the DL, which determines an acceleration of all dynamical processes described above. This phenomenon gives rise to an increase of the oscillation frequency, which is shown in Fig. 5. At a certain value of the current, the electron flux is large enough to sustain the simultaneous existences of both DLs in a stable state. The current jumps from the value corresponding to point f in the $I_E - V_E$ characteristic to the value corresponding to point g and becomes stationary. A further increase of V_{PS} leads to an increase of the diameter and the luminosity of the MDL. At a critical value of I_E the inner DL starts its dynamical behaviour, shown in the $I_E - V_E$ characteristic by the downward jump of the current h → i. The inner DL begins first because the current density through it is larger than that through the outer DL, inversely proportional to their surfaces areas. When the outer DL starts its own dynamical behaviour, I_E makes a new downward jump in the static characteristic (j → k in Fig. 2). At the beginning, the two dynamics are uncorrelated, which can explain the presence of flicker noise in the power spectrum (Fig. 6).

With the increase of V_E, also I_E increases (Fig. 2, branch k → l), and the two dynamics become correlated at a high-frequency and low amplitude (Figs. 3(vii) and 4 (vii), respectively). The above-described mechanism can also explain the appearance of other DL structures (as described in [26–28]) if the plasma density and the gas pressure are large enough. The hysteresis effect, which appears in the $I_E - V_E$ characteristic when V_E is gradually decreasing, proves that the DL can maintain its static or dynamic state under conditions lower than those required for the appearance of the respective state. In literature (see, e.g., [46]) it said that such a system possesses a special kind of memory of the past states.

To characterize the correlations, we have plotted the autocorrelation functions (see Fig. 10) corresponding to the signals from Fig. 3(vi) and (vii), respectively. From these functions we determined the autocorrelation time constant, defined as the time corresponding to the first zero (or the first local minimum) of the autocorrelation function. The obtained values prove that, at the beginning (Fig. 10(i)), the dynamics of the two DLs is uncorrelated ($\tau_c = 22\tau_s$, where τ_s is the sampling time of our acquisition data system, $\tau_s = 2\,\mu s$), and become more correlated ($\tau_c = 3\tau_s$) at high values of the voltage applied on the electrode (Fig. 10(ii)).

The frequencies of the observed two plasma states are so different because, according to Eq. (8):

$$\frac{f_1}{f_2} \cong \frac{\sigma_1}{\sigma_2}\sqrt{\frac{V_{DL1}}{V_{DL2}}} \tag{9}$$

Using our experimental data from Fig. 7, i.e., $V_{DL1} \cong 16$ and $V_{DL2} \cong 19\,V$ as the potential drops over the two DLs, and the values for $\sigma_{1,2}$ for 16 and 19 eV, respectively, again from [34], we obtain a theoretical ratio between the two frequencies of:

$$\frac{f_2}{f_1} \cong \frac{4 \times 10^{-17}}{2 \times 10^{-18}}\sqrt{\frac{19}{16}} \cong 22$$

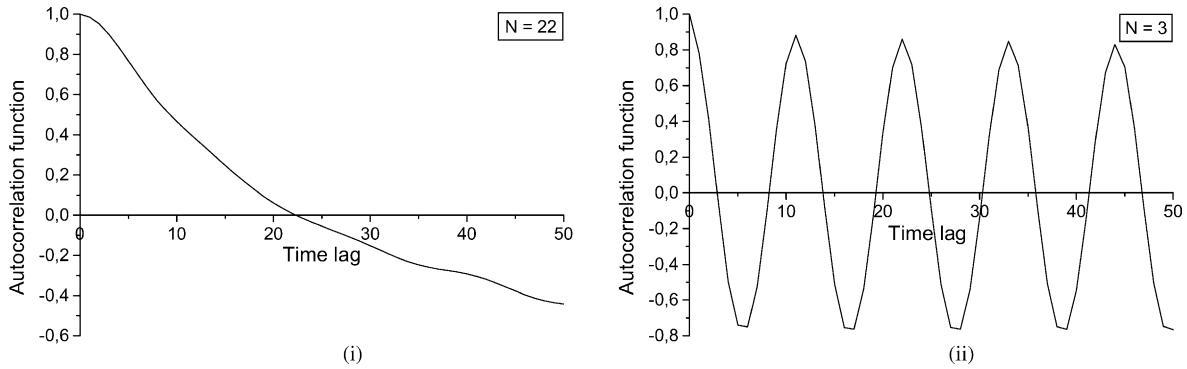

Fig. 10. Autocorrelation functions of the signals from Figs. 3(vi) and (vii), respectively.

Using the measured values of the frequencies we obtain:

$$\frac{f_2}{f_1} = \frac{40}{2.75} \cong 15$$

So, the theory predicts even a larger difference between the oscillation frequencies of the two DLs, forming together the MDL.

7. Conclusion

The experimental results yields evidence for the essential role of excitation and ionization processes for the generation and dynamics of a MDL in a plasma. The selected experimental geometry, with a positive biased electrode immersed in a steady state plasma, allows the identification of the mechanism, by which such a structure can exist in a plasma in stationary and dynamic states. The proposed mechanism sheds light on the role of the plasma density (which is determined by the discharge current) and the gas pressure in obtaining a MDL with a large number of plasma shells. The non-linear dynamical analysis of the signals gives us information about the attractors of the plasma system dynamic in the state space and about the Daubechies wavelet components on different octaves.

Acknowledgements

This work was supported by the Fonds zur Förderung der wissenschaftlichen Forschung (Austria) under grant no. P-14545-PHY and by the University of Innsbruck. The work of one of the authors (D.-G.D.) was carried out in the framework of ERASMUS-SOCRATES and CEEPUS programmes.

References

[1] R. Schrittwieser (Ed.), in: Proceedings of the Fourth Symposium on Double Layers and Other Nonlinear Potential Structures in Plasmas, Innsbruck, Austria, 1992, World Scientific Publishing Company, Singapore, 1993.
[2] S. Benkadda, T. Dudok de Wit, A. Verga, A. Sen, X. Garbet, ASDEX Team, Phys. Rev. Lett. 73 (1994) 3403.
[3] B.B. Kadomtsev, Rep. Prog. Phys. 59 (1996) 91.
[4] P.M. Bellan, Spheromaks, Imperial College Press, London, 2000.
[5] A.I. Kiryuskchenko, M.A. Lebedev, Sov. Phys. Tech. Phys. 16 (1971) 924.
[6] N. Sato, R. Hatakeyama, S. Iizuka, T. Mieno, K. Saeki, J.J. Rasmussen, P. Michelsen, R. Schrittwieser, J. Phys. Soc. Jpn. 52 (1983) 875.
[7] S. Iizuka, P. Michelsen, J.J. Rasmussen, R. Schrittwieser, R. Hatakeyama, K. Saeki, N. Sato, Phys. Rev. Lett. 48 (1982) 145; S. Iizuka, P. Michelsen, J.J. Rasmussen, R. Schrittwieser, R. Hatakeyama, K. Saeki, N. Sato, J. Phys. Soc. Jpn. 54 (1985) 2516.
[8] C. Avram, R. Schrittwieser, M. Sanduloviciu, J. Phys. D: Appl. Phys. 32 (1999) 2750, 2758.
[9] R. Schrittwieser, C. Avram, P.C. Balan, V. Pohoaţă, C. Stan, M. Sanduloviciu, Phys. Scripta T84 (2000) 122.
[10] R.T. Carpenter, S. Torvén, IEEE Trans. Plasma Sci. PS-15 (1997) 434.
[11] M. Temerin, K. Cerny, W. Lotko, F.S. Mozer, Phys. Rev. Lett. 48 (1982) 1175.
[12] R. Boström, IEEE Trans. Plasma Sci. 20 (1992) 756.
[13] H. Alfvén, P. Carlqvist, Sol. Phys. 1 (1967) 220.
[14] S. Singer, The Nature of Ball Lightning, Plenum Press, New York, 1971.
[15] M. Sanduloviciu, E. Lozneanu, J. Geophys. Res. 105 (2000) 4719.
[16] K.G. Emeleus, Int. J. Electronics 52 (1982) 407.
[17] B. Song, N. D'Angelo, R.L. Merlino, J. Phys. D: Appl. Phys. 24 (1991) 1789.
[18] M. Sanduloviciu, E. Lozneanu, Plasma Phys. Cont. Fusion 28 (1986) 585.
[19] E. Lozneanu, S. Popescu, M. Sanduloviciu, IEEE Trans. Plasma Sci. PS-30 (2002) 30.
[20] V. Pohoaţă, G. Popa, R. Schrittwieser, C. Ioniţă, M. Čerček, Phys. Rev. E 68 (2003) 16405.
[21] P. Coakley, N. Hershkowitz, Phys. Fluids 22 (1979) 1171.
[22] C. Chan, N. Hershkowitz, Phys. Fluids 25 (1982) 2135.
[23] A. Bailey, N. Hershkowitz, Geophys. Res. Lett. 15 (1988) 90.
[24] D. Diebold, C.E. Forest, N. Hershkowitz, M.-K. Hsieh, T. Intrator, D. Kaufman, G.-H. Kim, S.-G. Lee, J. Menard, IEEE Trans. Plasma Sci. PS-20 (1992) 601.
[25] T. Intrator, J. Menard, N. Hershkowitz, Phys. Fluids B 5 (1993) 806.
[26] L. Conde, L. León, Phys. Plasmas 1 (1994) 2441.
[27] O.A. Nerushev, S.A. Novopashin, V.V. Radchenko, G.I. Sukhinin, Phys. Rev. E 58 (1998) 4897.
[28] L. Conde, L. León, IEEE Trans. Plasma Sci. 27 (1999) 80.
[29] M. Sanduloviciu, E. Lozneanu, Plasma Phys. Cont. Fusion 28 (1986) 585.

[30] E. Lozneanu, C. Borcia, S. Popescu, M. Sanduloviciu, C. Avram, D. Dimitriu, V. Ignatescu, R. Schrittwieser, J. Plasma Fusion Res. Ser. 4 (2001) 331.
[31] S. Popescu, E. Lozneanu, M. Sanduloviciu, Chaos, Solitons Fractals 17 (2003) 203.
[32] H.L. Resnikoff, R.O. Wells, Jr., Wavelet Analysis, Springer-Verlag, 1998.
[33] I. Langmuir, Phys. Rev. 33 (1929) 954.
[34] D. Rapp, P. Englander-Golden, J. Chem. Phys. 43 (1965) 1464.
[35] B.N. Mandelbrot, J.R. Wallis, Water Resour. Res. 5 (1969) 321.
[36] P. Bak, C. Tang, K. Wiesenfeld, Phys. Rev. Lett. 59 (1987) 381;
P. Bak, C. Tang, K. Wiesenfeld, Phys. Rev. A 38 (1988) 364.
[37] M.A. Pedrosa, C. Hidalgo, B.A. Carreras, R. Balbin, J. Garcia-Cortés, D. Newman, B. van Milligen, E. Sánchez, J. Bleuel, M. Endler, S. Davies, G.F. Mattews, Phys. Rev. Lett. 82 (1999) 3621.
[38] N.H. Packard, J.P. Crutchfield, J.D. Farmer, R.S. Shaw, Phys. Rev. Lett. 45 (1980) 712.
[39] D. Ruelle, Chaotic Evolution and Strange Attractors, Cambridge University Press, 1989.
[40] F. Takens, in: D.A. Rand, L.S. Young (Eds.), Dynamical Systems and Turbulence, Lecture Notes Math. 898, Springer-Verlag, 1981.
[41] D.G. Dimitriu, V. Ignatescu, C. Ioniţă, E. Lozneanu, M. Sanduloviciu, R. Schrittwieser, Int. J. Mass Spectrom. 223/224 (2003) 141.
[42] A.H. Nayfeh, B. Balachandran, Applied Nonlinear Dynamics—Analytical, Computational and Experimental Methods, John Wiley & Sons, 1995.
[43] J.C. van den Berg (Ed.), Wavelets in Physics, Cambridge University Press, 1999.
[44] M. Strat, G. Strat, S. Gurlui, J. Phys. D: Appl. Phys. 32 (1999) 34.
[45] D. Alexandroaei, M. Sanduloviciu, Phys. Lett. A 122 (1987) 173.
[46] G. Nicolis, I. Prigogine, Exploring Complexity: an Introduction, W.H. Freeman & Co., New York, 1989.